Journal of African Earth Sciences 105 (2015) 17–28

Contents lists available at ScienceDirect

Journal of African Earth Sciences

journal homepage: www.elsevier.com/locate/jafrearsci

Geochemistry and potential environmental impact of the mine tailings at Rosh Pinah, southern Namibia

L. Nejeschlebová [a,f], O. Sracek [a,*], M. Mihaljevič [b], V. Ettler [b], B. Kříbek [c], I. Knésl [c], A. Vaněk [d], V. Penížek [d], Z. Dolníček [a], B. Mapani [e]

[a] Department of Geology, Faculty of Science, Palacký University, Olomouc, Czech Republic
[b] Inst. of Geochemistry, Mineralogy and Natural Resources, Faculty of Science, Charles University in Prague, Praha, Czech Republic
[c] Czech Geological Survey, Praha, Czech Republic
[d] Department of Soil Science and Soil Protection, Faculty of Agrobiology, Food and Natural Resources, Czech University of Life Sciences, Praha, Czech Republic
[e] University of Namibia, Windhoek, Namibia
[f] Inst. of Geology, Faculty of Science, Masaryk University, Brno, Czech Republic

ARTICLE INFO

Article history:
Received 7 November 2014
Received in revised form 14 February 2015
Accepted 17 February 2015
Available online 26 February 2015

Keywords:
Mine tailings
Neutral mine drainage
Oxyhydroxides
Carbonates
Barium
Gastric bioaccessibility

ABSTRACT

Mine tailings at Rosh Pinah located in semiarid southern Namibia were investigated by the combination of mineralogical methods and leaching using water and simulated gastric solution. They are well-neutralized with leachate pH > 7 and neutralization potential ratios (NPR) up to 4. Neutralization is mainly due to abundant Mn-rich dolomite in the matrix. Concentrations of released contaminants in water leachate follow the order Zn > Pb > Cu > As. Relatively high leached concentrations of Zn and partly also of Pb are caused by their link to relatively soluble carbonates and Mn-oxyhydroxides. In contrast, As is almost immobile by binding into Fe-oxyhydroxides, which are resistant to dissolution. Barium is released by the dissolution of Ba-carbonate (norsethite) and precipitates in sulfate-rich pore water as barite.

Dissolved concentrations in neutral mine drainage water collected in the southern pond are low, but when total concentrations including colloidal fraction are taken into account, more than 70% of Zn is in colloidal form. Groundwater upgradient of the mine tailings is of poor quality and there seems to be no negative impact on groundwater downgradient from mine tailings.

Contaminant concentrations in simulated gastric leachates are in the order Ba > Pb > Zn > Cu > As with a maximum gastric bioaccessibility of 86.6% for Ba and a minimum of 3.3% for As. These results demonstrate that total contaminant content and toxicity in the solid phase are poor predictors of risk, and therefore mineralogical and bioavailability/bioaccessibility studies are necessary for evaluation of contaminant environmental impact.

1. Introduction

Oxidation of sulfide minerals such as pyrite in mine tailings produces acidity and often results in acid mine drainage (Blowes et al., 2003). However, in some cases the neutralization capacity of the solid phase exceeds the acid production capacity and neutral mine drainage develops (Blowes et al., 1998; Romero et al., 2006). Under neutral pH and oxidizing conditions, sulfate concentrations are high, but dissolved ferric iron precipitates on the surface of sulfides where surface rims may limit oxidation of underlying sulfides (Nicholson et al., 1990; Hossner and Doolittle, 2003). Under neutral pH conditions, neutrophilic bacteria are more common than pyrite-oxidizing bacteria, which also slows sulfide oxidation (Blowes et al., 1998; Lindsey et al., 2009). Minerals precipitated under neutral conditions may form a hardpan layer, which limits penetration of oxygen and infiltration into mine tailings (McGregor and Blowes, 2002; Sracek et al., 2010a).

Under neutral conditions, dissolved metals and metalloids may precipitate or co-precipitate with hydroxides or in carbonates such as ferrihydrite, siderite, smithsonite, and cerussite. In such cases they can be efficiently immobilized in the solid phase and are not transported by water flowing out of mining wastes (Dold and Fontboté, 2001; Jamieson, 2011). However, when the contaminant bioaccessibility is estimated, the situation becomes more complex.

The term "bioaccessible fraction" is used for the amount of contaminant which is mobilized from the solid matrix under conditions prevailing in the human gastro-intestinal tract and

* Corresponding author.
E-mail addresses: ludmila.nejeschlebova@seznam.cz (L. Nejeschlebová), srondra@yahoo.com (O. Sracek).

http://dx.doi.org/10.1016/j.jafrearsci.2015.02.005
1464-343X/

"bioavailable fraction" is used for the fraction which can reach the blood stream (Ruby et al., 1999; Roussel et al., 2010). Several tests have been developed to test *in vitro* bioavailability of contaminants (Plumlee and Ziegler, 2006). A standardized test has been adopted by the US EPA (2007). Test results have indicated that some mineralogical forms of a contaminant, which are suitable for its immobilization in a solid matrix, may result in its high bioaccessibility (Jamieson, 2011). For example, at Montague gold district in Nova Scotia, Canada, high Ca/As mine tailings show a high dissolution rate of As-hosting Ca-bearing minerals (Meunier et al., 2010). In the Zambian Copperbelt, in the proximity of the copper smelter in Mufulira, the respective bioaccessibilities of Co and Cu in lateritic soils were up to 65% and 83% (Ettler et al., 2012). Romero et al. (2008) reported bioaccessibilities for Pb up to 20.5% in samples collected close to the smelter in San Luis Potosí, Mexico. These relatively low values were caused by the binding of Pb in sparingly soluble galena and anglesite. Dissolution kinetics may also play a role; e.g., two pools of Pb were suggested by Gasser et al. (1996) for samples from a site contaminated by Pb mining and processing. More than 50% of the Pb was released in initial 10 min, but the rest was released from 10 to 60 min at a much lower rate. This was interpreted as a consequence of Pb present in two different solid phase pools.

In arid to semi-arid conditions in the area of Rosh Pinah in southwestern Namibia, the mine tailings are a potential source of contamination. The neutral pH of the tailing results in precipitation of hydroxides and carbonates, which have relatively low solubility with a resulting low mobility of contaminants. In contrast, when these minerals are ingested, they become soluble in extremely acid gastric conditions. The aims of the present project were (a) geochemical and mineralogical characterization of mine tailings at Rosh Pinah, and (b) evaluation of their environmental impact, when an exposure pathway via surface and ground water and direct oral input of mine tailings material are considered. The impact of wind erosion and dust transport out of the mine tailings are discussed by Kříbek et al. (2014).

2. Study area

2.1. Site description, geology, and mining

The Rosh Pinah site is located in southwestern Namibia about 23 km north of the Orange River and about 100 km east of the Atlantic Ocean coast (Fig. 1a). The mine is operated by the Rosh Pinah Zinc Corporation (Pty) Ltd (RPZC). The RPZC mine is located south of the Rosh Pinah Mountains. The town Rosh Pinah lies northwest of the mine tailings, (Fig. 1b), at the border of a valley trending NW–SE, and has a population of 4,300 while the adjacent Tutungeni settlement hosts 3,500 people. More than half of the total population consists of employees of the two local zinc mines (at RPZC and Skorpion) and their families.

The 740 Ma syngenetic Rosh Pinah zinc-lead ore deposit is classified as sedimentary-exhalative (SEDEX) type (Alchin et al., 2005; van Vuuren, 1986). The ore zone is composed of disseminated to massive sulfides, with sphalerite (ZnS), galena (PbS), pyrite (FeS_2), and chalcopyrite ($CuFeS_2$) as the principal sulfide minerals. The strata-bound mineralization is located in silicified black shale,

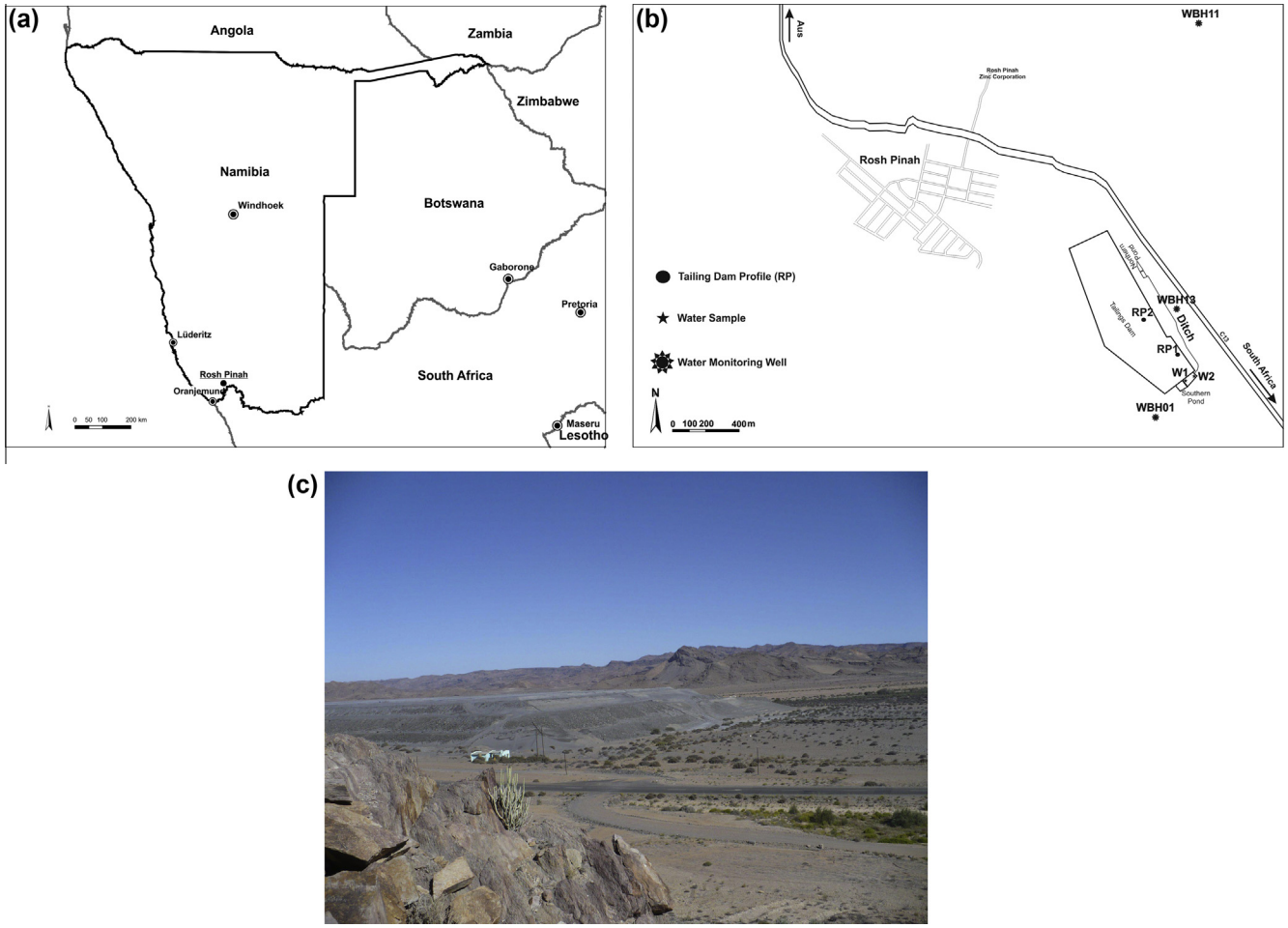

Fig. 1. (a) Location of Rosh Pinah, (b) mine tailings and sampling sites, (c) view of mine tailings from the northeast.

feldspar-bearing arenites and altered carbonate rocks of the Neoproterozoic Rosh Pinah Formation in the Port Nolloth Zone (Alchin et al., 2005). There is also a significant barium enrichment linked to norsethite ($BaMg(CO_3)_2$) and barite ($BaSO_4$).

The Rosh Pinah mine has been operated for 47 years and 23 Mt of ore at 7.9% Zn, 1.7% Pb and 0.14% Cu were extracted from 1969 to 2013. The current ore production is 700,000 ton per year. Ores from various ore bodies and levels are mixed and crushed underground to less than 150 mm in diameter. The crushed and pulverized fraction (<120 μm) is treated in the flotation ore treatment plant, where Pb and Zn concentrates are produced. Dried concentrates are transported by trucks to Lüderitz harbor from where they are exported overseas. Tailings from thickeners are pumped and transported via 1.5 km long pipe. The mine tailings dam (Fig. 1b, c) is located about 1.5 km south of the ore treatment plant and about 500 m SE of the town of Rosh Pinah. Currently, the mine tailings cover an area of 60 hectares and are more than 25 m high.

2.2. Climate and soils

The local climate is arid with a very irregular distribution of precipitation. The rainy season is between April and September, i.e., during the winter. The average annual rainfall is 64.6 mm and the annual potential evaporation is 875 mm. Temperatures in summer vary from 30 to 40 °C, while in winter they vary between 20 and 25 °C.

Climatic conditions result in the formation of thin Leptosols, which develop directly on weathered rock material. Soils developed on the sediments which have been transported by runoff after rare intensive rains in the valley bottom are relatively thick, have a coarse texture, and are classified as Haplic Regosols or Haplic Arenosols. Their pH is in the alkaline range and the soils are characterized by high contents of sodium, high salinity, and relatively low contents of clay fraction (ASEC, 2005).

3. Material and methods

3.1. Sampling of mine tailings and water

Sampling profile RP1 was located at a topographic elevation in the south of mine tailings (Fig. 1b). Sampling profile RP2 was on the top plateau north of RP1 (Fig. 1b). Both profiles were dry during sampling, but RP2 showed a higher water content. At both sampling sites, the tailings material is relatively fresh, about 1 year old on the top of the profiles. There was no vegetation at either sampling site. Samples of tailings solids were obtained down to a depth of 2.4 m using a hand drilling auger with an inner diameter of 4 inches. The samples were packed in polyethylene (PE) bags. Mine drainage water was sampled from the southern pond (Fig. 1b). Field parameters T, pH, Eh, and EC were measured on-site. Water was filtered through 0.45 μm filters, then acidified for cation and trace elements analyses by HNO_3 and collected in PE bottles. Simultaneously, a second water sample was only acidified, but not filtered to determine the difference between dissolved and colloidal trace element concentrations. Samples for anion analyses were filtered, but not acidified. Groundwater analyses data for monitoring wells were provided by Ms. Gisela Hinder from the Rosh Pinah mine.

3.2. Bulk composition of solid samples

The pseudo-total digests of samples were obtained by a standardized *aqua regia* extraction protocol in accordance with the ISO 11466 procedure (International Organization for Standardization 1995). All reagents were declared *pro analysi*, and all solutions were prepared using double-distilled water. Standard working solutions were prepared from original certified stock solutions (MERCK) of concentration 1,000 mg l^{-1} in 1% super pure HNO_3. Heavy metals and metalloids were determined using Flame Atomic Absorption Spectroscopy (FAAS, Perkin Elmer 4000 Spectrometer). Certified reference material (CRM 7001, sandy soil) was used to control the accuracy of the *aqua regia* pseudo-total digestion, yielding reproducibility values below 10%. Total sulfur (S_{tot}) was determined using the ELTRA CS 500 instrument. Samples were combusted at a temperature of 1400 °C, and the S_{tot}, measured as released SO_2, was determined by an IR detector. The detection limits used for S_{tot} were 0.01 wt.%. Relative errors of S_{tot}, determined using reference materials (CRM 7001), were ±2.5%. Inorganic C was determined using a Leco elemental analyzer. Total S and inorganic C were used in acid–base accounting (ABA) to calculate acid potential (AP), neutralization potential (NP) and neutralization potential ratio (NPR) using the modified method of Sobek (Jambor, 2003). Sequential extraction data (see later) were used to correct AP for the presence of acid not producing sphalerite and NP for the presence of norsethite.

3.3. X-ray powder diffraction (XRD) of heavy fractions of sediments

The XRD analyses were performed with a Philips X'Pert instrument (Co Kα, 40 kV/40 mA) equipped with an X'Celerator detector and programmable incident and diffracted beam anti-scatter slits. Samples were placed on zero-background Si slides, gently pressed in order to obtain sample thicknesses of about 0.5 mm and scanned at a near constant irradiation volume in the 2θ range of 3°–65° in steps of 0.017° for 5.83 s per step. Results were interpreted by the program ZDS (Ondruš, 1993). Heavy minerals in each sample were concentrated by separation in 1,1,2,2-tetrabromomethane before analyses.

3.4. Electron microprobe

Several solid phase samples were also studied with an electron microprobe (EMP), using a CAMECA SX100 apparatus, equipped with five crystal spectrometers and an energy dispersive X-ray spectrum (EDS) analyzer. The analyses were performed at an accelerating voltage of 15 kV, a probe current of 10–20 nA, a spot size of 5 μm, and a counting time of 10–30 s, with natural and synthetic standards, using the PAP correction procedure.

3.5. Sequential extraction

Sequential extractions for selected bulk sediment samples were performed using the BCR procedure (Rauret et al., 1999). The following extraction scheme was used: a 0.11 M acetic acid (CH_3COOH) step targeting exchangeable and acid soluble fractions; a 0.5 M hydroxylamine-hydrochloride ($NH_2OH{\cdot}HCl$) step targeting the reducible fraction (mostly poorly crystalline iron/manganese oxides); an oxidizable step (8.8 M H_2O_2/1 M CH_3COONH_4 extractable) targeting organic matter and sulfides; and an *aqua regia* step targeting the residual fraction. The detailed experimental scheme is given by Rauret et al. (1999).

3.6. Water leaching of samples

Since no water was recovered from the mine tailings, 50 g of homogenized sample were suspended in 150 ml of deionized water and agitated on a rotary shaker until stable readings of pH and electrical conductivity (EC) were obtained. After stabilization of pH and EC, the leachate was decanted and filtered through a 0.45 μm filter and then split into one subsample acidified with ultrapure HNO_3 for determination of cations and metals, and a second non-acidified subsample. Cations and metals were determined

by FAAS (Varian AA 280 FS) under standard analytical conditions. Arsenic was determined by ICP MS. The analytical precision of the individual analyses was below 2%. Standard reference materials BCR 483 (soil) and BCR 701 (sediment) were used for quality control of analytical data. Anions were determined by HPLC (Dionex ICS 2000). Alkalinity was determined by titration with HCl using the Gran plot to determine the end point. Water samples from the southern pond were analyzed by the same methods as water leaching samples.

3.7. Gastric leaching of samples

The bioaccessibility test, which simulates conditions in the human gastric tract, was performed following the US EPA (2007) protocol. The extraction liquid contained 0.4 M glycine (i.e. 30.028 g glycine/800 ml deionized water) adjusted to a pH of 1.5 by pure grade HCl and finalized to 1 l by deionized water (MilliQ+). The ratio solid to fluid was 0.01 and 0.5 g of samples were placed in 50 ml of extraction fluid and agitated for 2 h at a body temperature of 37 °C. The extract was filtered through 0.45 μm filter and analyzed for Zn, Pb, Cu, Co, Cd, and As by ICP-MS. Bioaccessible concentrations were expressed in mg/kg (ppm) and converted to% of total content.

3.8. Geochemical modeling

Speciation calculations were performed by the program PHREEQC (Parkhurst and Appelo, 1999) using the database minteq.dat.

4. Results

4.1. Solid phase composition and mineralogy

Bulk solid phase contents are in the order Fe > Zn > Mn > Ba > Pb > Cu > As, which seems to be related mainly to the depositional environment and are shown for selected elements in Fig. 2.

Contents of Cu in the profile RP1 (average 781.7 ppm, standard deviation 330.7 ppm) reach 1,680 ppm at the surface of the mine tailings and then drop below 1,000 ppm at depth except sample at 1.9 m with a content of 1,132 ppm (Fig. 2a). In the profile RPT2 (average 690 ppm, standard deviation 334.9 ppm), a maximum of 1,553 ppm is located at 1.1 m depth and most contents vary between 385 ppm and 1,080 ppm.

Contents of Pb are generally higher than those of Cu with respective maximum values of 2,360 ppm at 0.5 m in the profile RPT1 (average 892.8 ppm, standard deviation 595.8 ppm), and 2,215 ppm at 1.1 m in the profile RPT2 (average 625.1 ppm, standard deviation 530.2 ppm) (Fig. 2a).

Contents of As are in the range 100–200 ppm in the profile RPT1 (average 151.2 ppm, standard deviation 36.7 ppm) except a value of 236 ppm at 0.3 m depth. In the profile RPT2 (average 116.1 ppm, standard deviation 44.8 ppm) the range of values is similar and a maximum of 256 ppm is located at 1.1 m depth (Fig. 2a).

Contents of Fe in the profile RPT1 (average 37,846 ppm, standard deviation 11,421.5 ppm) reach almost 60,000 ppm close to surface and then drop with depth to about 40,000 ppm. In the profile RPT2 (average 30,906.9 ppm, standard deviation 7,449.6 ppm), values are lower, with a maximum 48,400 ppm at 1.1 m depth (Fig. 2b).

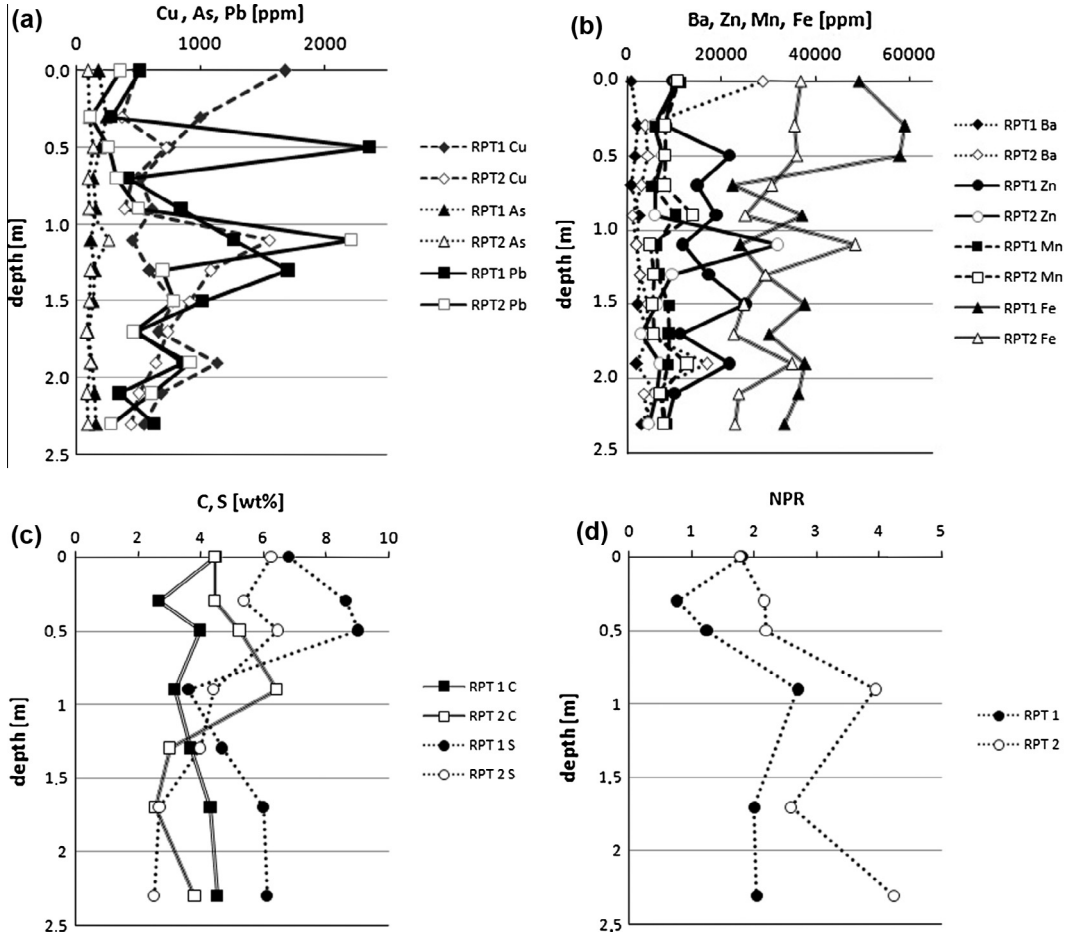

Fig. 2. Bulk contents in solid phase: (a) Cu, As, Pb, (b) Ba, Zn, Mn, Fe, (c), C, S, (d) neutralization potential ratio (NPR).

Contents of Mn in the profile RPT1 (average 7,847.5 ppm, standard deviation 1,691.9 ppm) reach 11,233 ppm at surface, but generally are from 5,000 to 6,000 ppm. In the profile RPT2 (average 8,120.7 ppm, standard deviation 2,818.5 ppm), a maximum of 14,020 ppm is located at 0.9 m depth and most values are between 5,000 and 10,000 ppm (Fig. 2b).

Contents of Zn in the profile RPT1 (average 14,926.9 ppm, standard deviation 5,645.5 ppm) reach more than 20,000 ppm with a maximum of 21,683 ppm at 0.5 m depth. In the profile RPT2, Zn contents vary between 4,500 ppm and 10,500 ppm except a value of 32,013 ppm located at 1.1 m depth (Fig. 2b).

Contents of Ba in the profile RPT1 (average 2,471.9 ppm, standard deviation 1,440.7 ppm) vary between 700 and 6,040 ppm and a maximum is at 2.1 m depth. Maximum contents in the profile RPT2 (average 6,567.2, standard deviation 7,754.1 ppm) are significantly higher, reaching 28,820 ppm at the surface and 16,840 ppm at 1.9 m depth. Other contents are between 1,000 ppm and 4,600 ppm (Fig. 2b).

Contents of total S vary between 2.2 and 9.6 wt.% (Fig. 2c). Maximum values at both profiles are at depths < 0.5 m. Values of inorganic C are between 2.4 and 6.1 wt.%. In the profile RPT1 they are high close to surface and then they decrease. In contrast, in the profile RPT2 there is a slight increase with depth (Fig. 2c).

Values of neutralization potential ratio (NPR) calculated by the modified method of Sobek are reported in Fig. 2d. Sulfur linked to acid not producing sphalerite was subtracted from AP on the basis of Zn in the oxidizable step of sequential extraction using stoichiometric ratios Zn/S 1:1 and inorganic carbon linked to norsethite was subtracted from NP on the basis of the acid extractable step of sequential extraction using a stoichiometric ratio Ba/C 1:2. All values except one are higher than 1.0, i.e., indicating that there is no generation of acid mine drainage, only one sample from the RPT1 profile located at 0.3 m depth shows a value of 0.77. A maximum value of 4.23 was determined in the profile RPT2 at 2.3 m depth. However, the values represent a worst case scenario because a non-negligible fraction of total S is probably already present in sulfate minerals (e.g. gypsum) and does not contribute to the generation of acidity.

Table 1
Relative abundance of minerals based on X-ray diffraction of fraction separated in 1,1,2,2-tetrabromethane (1 – least abundant, 5 – most abundant).

Sample	RPT 1			RPT 2		
Depth (cm)	0–20	100–120	220–240	0–20	100–120	220–240
Dolomite	5	5	5	5	4	5
Sphalerite	4	3	2	2	5	3
Pyrite	4	3	3	3	4	3
Barite	3	3	4	3	3	2
Norsethite	3	3	2	1	1	1
Pyrrhotite	n.f.	n.f.	n.f.	n.f.	1	1
Quartz	2	2	1	2	1	2
Biotite	1	n.f.	n.f.	n.f.	n.f.	n.f.
Calcite	1	n.f.	n.f.	1	1	n.f.
Gypsum	1	n.f.	n.f.	n.f.	1	n.f.
Orthoclase	n.f.	1	1	n.f.	1	n.f.

n.f. – not found.

Relative abundances of minerals in the heavy fraction separated in 1,1,2,2-tetrabromomethane are reported in Table 1 and representative X-ray diffraction patterns are presented in Fig. 3. The principal primary gangue mineral is dolomite, but traces of calcite were also found. Other primary minerals are K-feldspar and biotite. Primary sulfides include sphalerite and pyrite and trace amounts of pyrrhotite. There are relatively high amounts of Ba-minerals norsethite and barite. Gypsum was found only in small amounts. On the other hand, no crystalline ferric oxyhydroxides were detected by X-ray diffraction, suggesting their amounts are below the detection limit. The X-ray diffraction patterns for samples from the profile RPT1 (Fig. 3a) and the profile RPT 2 (Fig. 3b) were similar, but in the latter only relatively small amounts of calcite and gypsum were found.

Electron microprobe images in back-scattered electron mode are shown in Fig. 4. In Fig. 4a, the grain of sphalerite is surrounded by a matrix of ferric oxyhydroxides of goethite composition. The grain is coated by oxyhydroxide rims. Based on the EDS analysis, the goethite contains 0.73 wt.% of Zn. In the matrix, there is primary muscovite and secondary gypsum. In Fig. 4b, sphalerite is also present plus pyrite and gypsum has precipitated on the surface of dolomite, which is rich in Mn. Other primary minerals are represented by quartz and Ba-rich feldspar as well as norsethite.

4.2. Sequential extraction

In the sequential extraction of Fe, the order of fractions is *aqua regia* > oxidizable > reducible > acid extractable (Fig. 5a). Maximum total contents occur in the RPT1 profile at 0.4 m and

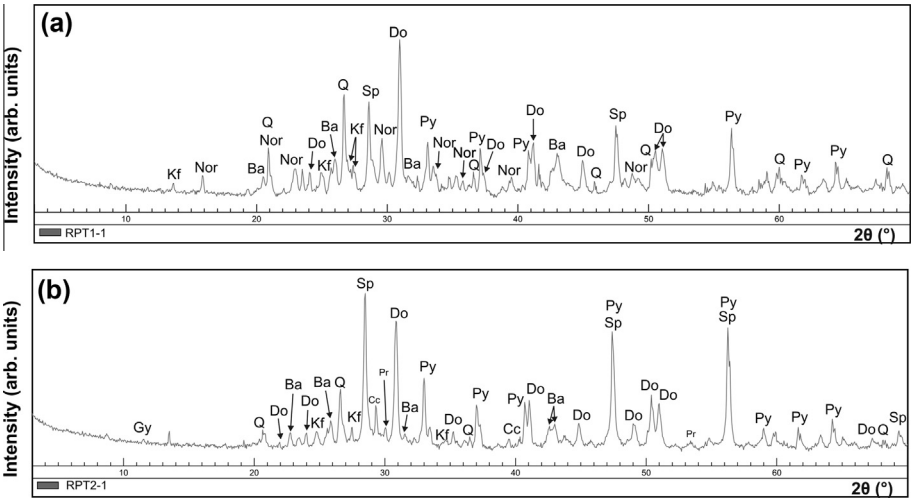

Fig. 3. X-ray diffraction patterns: (a) RP1, (b) RP2, each sample is from 1.0 m depth, legend: Q – quartz, Plq – plagioclase, Kf – K-feldspar, Nor – norsethite, Py – pyrite, Pr – pyrrhotite, Ba – barite, Sp – sphalerite, Cc – calcite, Do – dolomite.

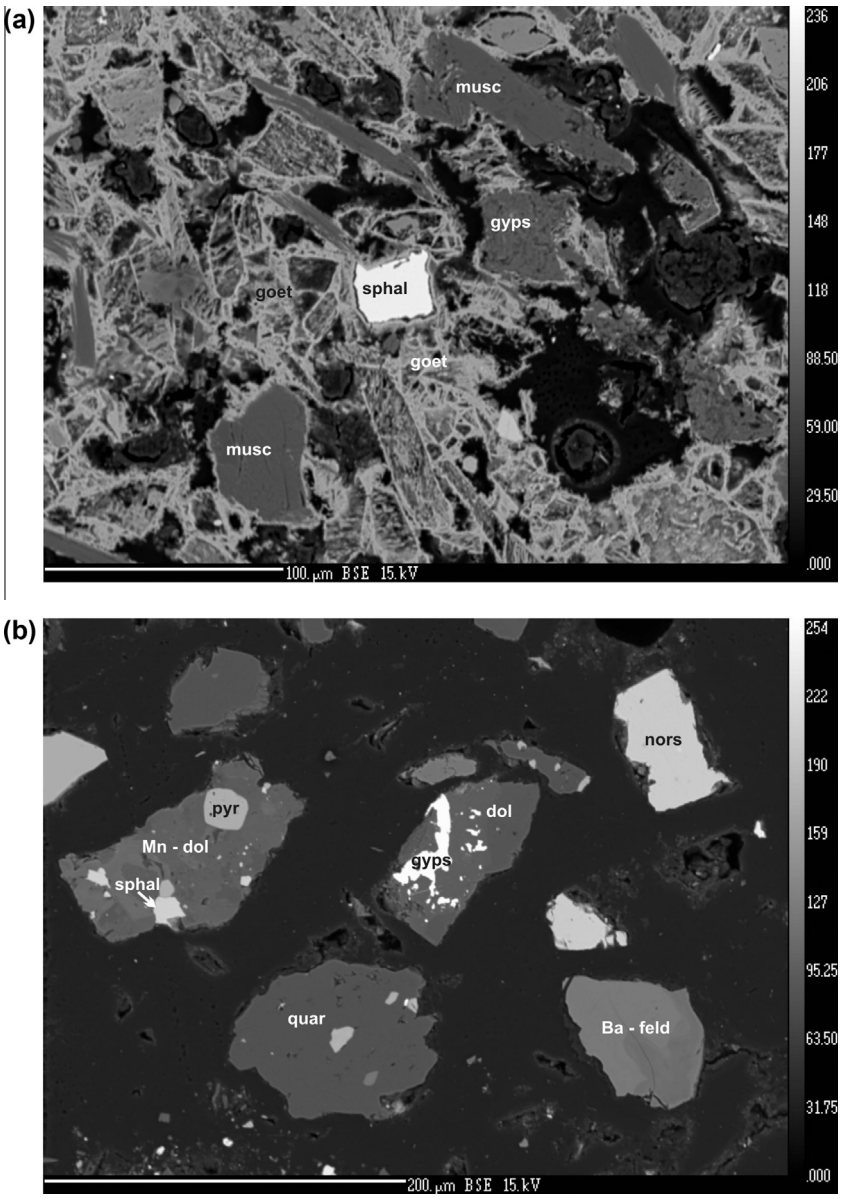

Fig. 4. EMP images, sphal-sphalerite, gyps-gypsum, goet-goethite, musc-muscovite, dol-dolomite, pyr-pyrite, nors-norsethite, quar-quartz.

0.6 m depth, where they reach more than 50,000 ppm. In the profile RPT2, contents are lower with a maximum about 34,000 ppm at 0.6 m depth. Dominance of the *aqua regia* fraction suggests fast transformation of low crystallinity ferric phases to crystalline phases such as goethite. The oxidizable fraction corresponds to abundant unoxidized Fe-sulfides.

The order of fractions for Mn is acid extractable ≅ reducible > oxidizable > *aqua regia* (Fig. 5b). A maximum of about 11,700 ppm was found in the profile RPT2 at 1.0 m depth, but contents >6,000 ppm are common in most samples. The acid extractable fraction seems to correspond to Mn in carbonates such as Mn-rich dolomite and rhodochrosite. However, a large amount of Mn is also present in the oxide and hydroxides as indicated by a large reducible fraction.

For Zn, the order of fractions is oxidizable > *aqua regia* > acid extractable > reducible with a maximum of about 20,000 ppm in the profile RPT1 at 0.6 m depth (Fig. 5c). In the profile RPT2, contents are less than 10,000 ppm elsewhere. The oxidizable fraction corresponds to sphalerite, but Zn in carbonates, probably smithsonite, is also present as suggested by the acid extractable fraction.

For Pb, the order of fractions is *aqua regia* > acid extractable > oxidizable ≅ reducible (Fig. 5d). Contents are lower than those of zinc and reach a maximum of more than 5,200 ppm in the RPT1 at 0.6 m depth. A maximum of about 3,900 m in the profile RPT2 is found at 0.6 m depth. Similar to Zn, the oxidizable fraction corresponds to unoxidized galena and the acid extractable fraction to Pb bound in carbonates.

The order of fractions for Cu is oxidizable > *aqua regia* > acid extractable > reducible (Fig. 5e). A maximum of 1,600 ppm is found in the profile RPT1 at 0.2 m depth. In the profile RPT2, contents are significantly lower with a maximum of about 640 ppm at 1.8 m depth. A dominance of the oxidizable fraction suggests the presence of unoxidized Cu-sulfides such as chalcopyrite, but carbonates represented by the acid extractable fraction are also present.

The order of fractions for As is *aqua regia* > oxidizable > reducible > acid extractable (Fig. 5f). A maximum of about 160 ppm is in the profile RPT1 at 0.6 m depth. In the profile

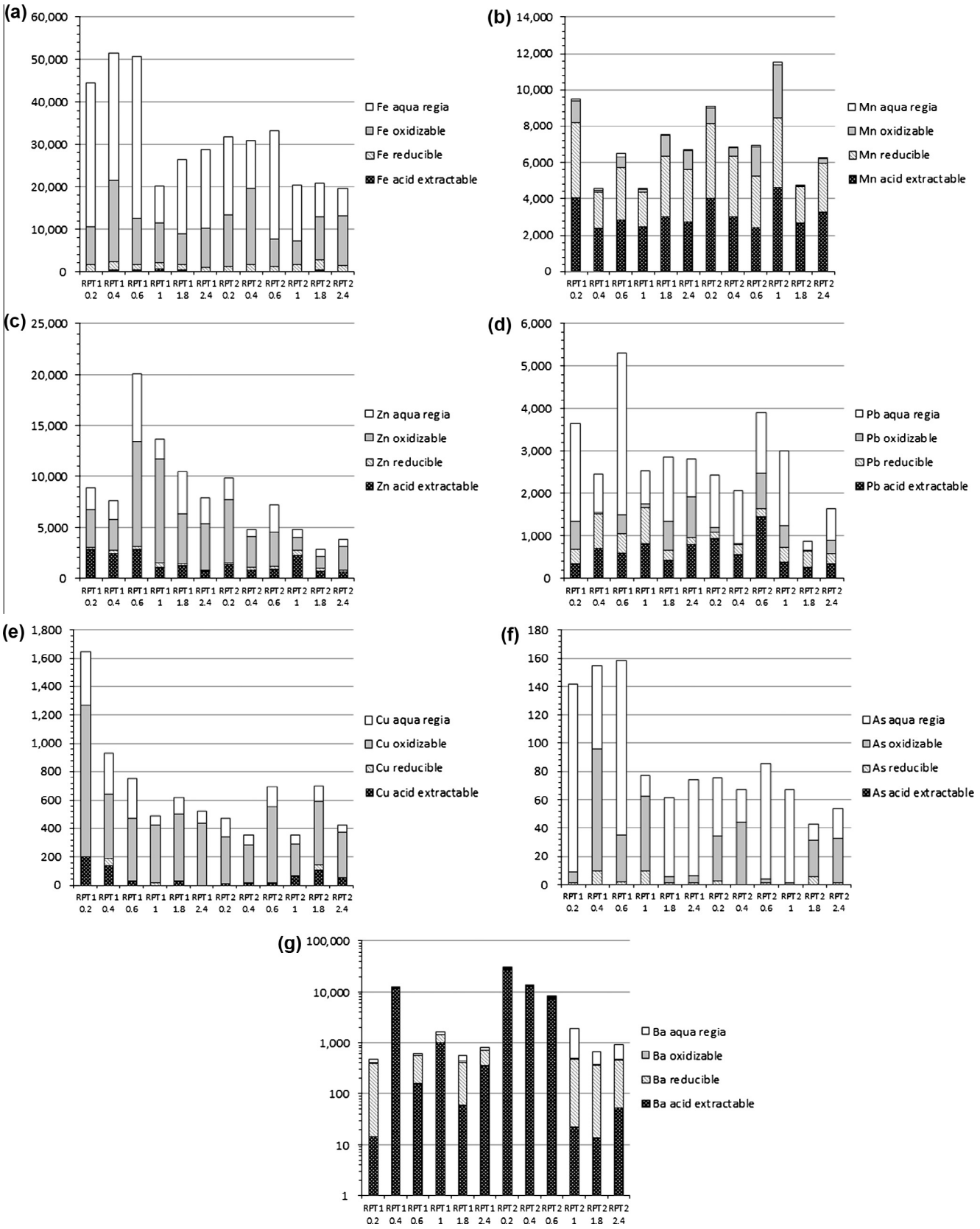

Fig. 5. Sequential extraction results, contents in ppm: (a) Fe, (b) Mn, (c) Zn, (d) Pb, (e) Cu, (f) As, (g) Ba.

RPT2, a maximum of about 90 ppm is also at 0.6 m depth. In the *aqua regia* fraction, arsenic is probably bound in highly crystalline ferric oxide and hydroxides. In the oxidizable fraction, arsenic is still in primary sulfides such as As-pyrite.

Finally, the order of fractions for Ba is acid extractable > reducible > *aqua regia* > oxidizable (Fig. 5g). A maximum of more than 30,000 ppm was located in the profile RPT2 at 0.2 m depth, but contents more than 10,000 ppm occur in several samples. It seems that most of the Ba is present in Ba-carbonate norsethite, which is very common in the Rosh Pinah mine tailings and dissolves mainly in the acid extractable step.

4.3. Water chemistry

Sampled profiles in the mine tailings were completely dry. There was water discharging directly from the base of the mine tailings and collected in the southern pond (Fig. 1b). Samples RP-w1 a RP-w2 showed pH values of 7.03 and 7.45, respectively (Table 2). Waters had relatively low mineralization (electrical conductivity values were 0.913 and 0.918 mS/cm, respectively) and concentrations of sulfate were less than 100 mg/l. Dissolved concentrations of Zn, Pb and Cu were up to 196 μg/l, 91 μg/l, and 790 μg/l, respectively. However, when unfiltered acidified samples were analyzed, respective concentrations increased to 736 μg/l, 178 μg/l and 863 μg/l. This indicates the presence of colloids with a maximum value of 73.4% of the total concentration for Zn and a minimum value of 8.5% of the total concentration for Cu. Concentrations of Ba were up to 299 μg/l, but the colloidal fraction was negligible.

Table 2
Water chemistry from pond and groundwater wells, f – filtered, n – not filtered, n.a. – not available.

Parameter	RP-1w-f	RP-2w-f	RP-1w-n	RP-2w-n	WBH01	WBH13	WBH11
pH	7.03	7.45	–	–	7.9	7.8	7.6
T (°C)	18.2	18.1	–	–	n.a.	n.a.	n.a.
EC (mS/cm)	0.913	0.918	–	–	4.11	2.49	8.28
Na (mg/l)	101	97	–	–	480	250	680
K (mg/l)	0.33	0.34	–	–	25	11	36
Ca (mg/l)	30	30	–	–	261	128	673
Mg (mg/l)	29.7	28.8	–	–	135	77	432
Alkalinity (mg/l as HCO_3)	201	217	–	–	254	176	185
SO_4 (mg/l)	95	94	–	–	1,330	320	1,980
Cl (mg/l)	68.6	75.1	–	–	380	420	1,640
F (mg/l)	1.1	0.9	–	–	1.1	1.4	1
Fe (μg/l)	65.5	63.2	398	364	40	<10	<10
Mn (μg/l)	579	576	805	795	10	10	280
Al (μg/l)	9.9	6.3	289	246			n.a.
Zn (μg/l)	196	153	460	736	130	110	160
Pb (μg/l)	91	88	142	178	<20	<20	<20
Cu (μg/l)	790	799	855	863	70	30	40
Co (μg/l)	3.2	3.1	3.2	3.3	n.a.	n.a.	n.a.
Cd (μg/l)	0.56	0.43	1.1	1.6	<10	<10	<10
As (μg/l)	4.3	4.1	5.5	5.2	<10	<10	<10
Ba (μg/l)	295	299	295	334	n.a.	n.a.	n.a.

Groundwater from well WBH11 located upgradient from the mine tailings (Fig. 2) seems to represent mountain front recharge in arid regions and has much higher mineralization (electrical conductivity 8.28 mS/cm) than samples discharged from mine tailings, with respective concentrations of SO_4 and Cl of 1,980 mg/l and 1,640 mg/l. Samples from monitoring wells WBH01 and WBH13 close to the mine tailings (Fig. 1b) had similar chemistry like well WBH11, but concentrations were lower. Most trace metals showed concentrations below detection limits; just detectable Zn and Cu concentrations were similar to those in samples of the mine tailings discharge. This suggests that there is no contamination of groundwater linked to the mine tailings and groundwater is already of poor quality upgradient of the studied site. However, number of sampled wells is limited and more detailed monitoring would be necessary to confirm it.

Saturation indices for relevant minerals are reported in Table 3. Samples from the southern pond are supersaturated with respect to barite, $Fe(OH)_3(a)$, goethite, and manganite. They also are supersaturated or slightly undersaturated with respect to rhodochrosite, but saturation is not reached for calcite and dolomite, any Zn- and Pb-carbonates, or for gypsum. High calculated values of log P_{CO2} (>−2.0 at the inflow of pond) are a consequence of carbonate neutralization in mine tailings followed by slow de-gassing of CO_2 in the pond.

Groundwater samples are supersaturated with respect to calcite and dolomite. Saturation is not reached for gypsum, but groundwater sample WBH13 is close to saturation. Calculated log P_{CO2} values are much lower than those for pond samples.

4.4. Water leachates

In general, all leachate pH values are in the alkaline region and leached concentrations are in the order Zn > Mn > Fe > Pb > Cu > Ba > As, in good agreement with the mineralogy.

Values of leachate pH are always > 7.0, (Fig. 6a), and for samples from the profile RPT1 they increase from 7.16 at shallow depth to 7.91 at 1.3 m depth and then slightly decrease. For the profile RPT2, a minimum of 7.17 is located at 1.3 m depth and a maximum of 7.74 is located at 0.3 m depth.

Concentrations of Cu in leachates in the profile RPT1 are between 3 and 36 ppb (Fig. 6b) with a maximum at 0.5 m depth. In the profile RPT2 they are slightly higher, from 5 to 67 ppb and the maximum is at 1.7 m depth. Concentrations of As are very low (Fig. 6b), in samples from profile RPT1 they vary from 0.1 to 5 ppb with a maximum at surface. In the profile RPT2, water-leached As concentrations are only from 0.1 to 1.6 ppb and the maximum is also found in the surface sample. Concentrations of Pb are higher (Fig. 6b), in the range 77–155 ppb in the profile RPT1 with a maximum at surface. In the profile RPT2, the Pb range is from 45 to 126 ppb with a maximum also at surface.

Concentrations of leached Zn are high (Fig. 6c), in the profile RPT1 they vary from 2,100 to 10,390 ppb with a maximum at surface. In the profile RPT2 the range is from 860 to 15,160 ppb and the maximum is also at surface. Water-leached Mn concentrations in the profile RPT1 vary from 790 to 7,990 ppb, with a maximum at

Table 3
Saturation indices for selected minerals and log P_{CO2} values.

SI value/sample	Calcite	Dolomite	Cerussite	Smithsonite	Barite	$Fe(OH)_3(a)$	Goethite	Gypsum	Manganite	Rhodochrosite	Log P_{CO2}
RP-1w	−0.81	−1.33	−0.47	−1.86	0.91	1.84	7.47	−2.01	4.65	−0.07	−1.77
RP-2w	−0.36	−0.46	−0.45	−1.62	0.90	2.0	7.64	−2.0	5.47	0.34	−2.18
WBH01	0.81	1.60	n.a.	−1.58	n.a.	1.75	7.45	−0.42	−1.33	−1.21	−2.61
WBH11	0.42	0.91	n.a.	−1.66	n.a.	n.a.	n.a.	−1.12	−1.57	−1.28	−2.64
WBH13	0.67	1.45	n.a.	−1.84	n.a.	n.a.	n.a.	−0.10	−0.93	−0.24	−2.52

n.a. – not available, a component of mineral either was not determined or was below detection limit.

surface (Fig. 6c). In the profile RPT2, Mn concentrations are in the range 400–12,510 ppb and a maximum is at 0.7 m depth. Concentrations of leached Fe are much lower than those of Mn (Fig. 6c), in the range 610–1,090 ppb in the profile RPT1. In the profile RPT2, they vary from 430 to 1,200 ppb and the maximum is at 1.7 m depth.

Concentrations of leached Ba in the profile RPT1 are in the range 9–18 ppb and the maximum is at surface (Fig. 6c). In the profile RPT2 the Ba concentrations are from 12 to 36 ppb and the maximum is also at surface. Concentrations of Ca in the profile RPT1 are from 284 to 603 mg/l (Fig. 6d) with maximum values at shallow depth. In the profile RPT2, the values are from 229 to 639 mg/l and the maximum is at 1.7 m depth. Finally, concentrations of SO_4 in the profile RPT1 are from 165 to 266 mg/l with a maximum at surface, (Fig. 6d), and in the profile RPT2 they vary from 121 to 244 mg/l with a maximum at 0.7 m depth.

4.5. Gastric leachates

Gastric leaching concentrations based on samples from the surface of mine tailings for contaminants of interest are shown in Fig. 7 and Table 4. The order was Ba > Zn > Pb > Cu > As with a maximum of 21,400 ppm for Ba at profile RPT2. Maximum contents of Zn and Pb mobilized in simulated gastric acid were about 4,160 and 299 ppm, respectively (Fig. 7a). Mobilized contents for Cu and As were significantly lower, with maximum values of 297 ppm and 6 ppm, respectively (Fig. 7b, Table 4). When contents mobilized in simulated gastric fluid are compared with total contents in the samples, maximum bioaccessible fractions (BAF) of 86.6% is found for Ba in the profile RPT1. For Pb in the profile RPT2 maximum BAF is 72.0%. A relatively low BAF value (3.3%) was found for As (Table 4).

5. Discussion

The mine tailings at Rosh Pinah are well-neutralized with corrected neutralization potential ratio (NPR) generally higher than one and reaching 4.0 for some samples. This is in a good agreement with leachate pH values ranging from 7.16 to 7.91 and with relatively high dissolved concentrations of Ca (>600 mg/l) (Fig. 6d). Similar neutralization behavior was recently reported for the mine tailings in the Zambian Copperbelt, where NPR values are even higher (Sracek et al., 2010a). The principal neutralization mineral at Rosh Pinah is Mn-rich dolomite. Acid–base accounting (ABA) is subjected to some uncertainty and results must be interpreted with caution (Lindsey et al., 2009), e.g., at Rosh Pinah inorganic C may be partly present in Ba-carbonate, norsethite, and may not contribute to the neutralization. The principal sulfide mineral of zinc is sphalerite, but its dissolution does not produce acidity, just dissolved zinc and sulfate (Dold, 2010):

$$ZnS + 2O_2 = Zn^{2+} + SO_4^{2-} \quad (1)$$

The ABA was corrected for the presence of sphalerite and norsethite on the basis of sequential extraction data. However, a part of S is present in gypsum and the resulting acid potential based on

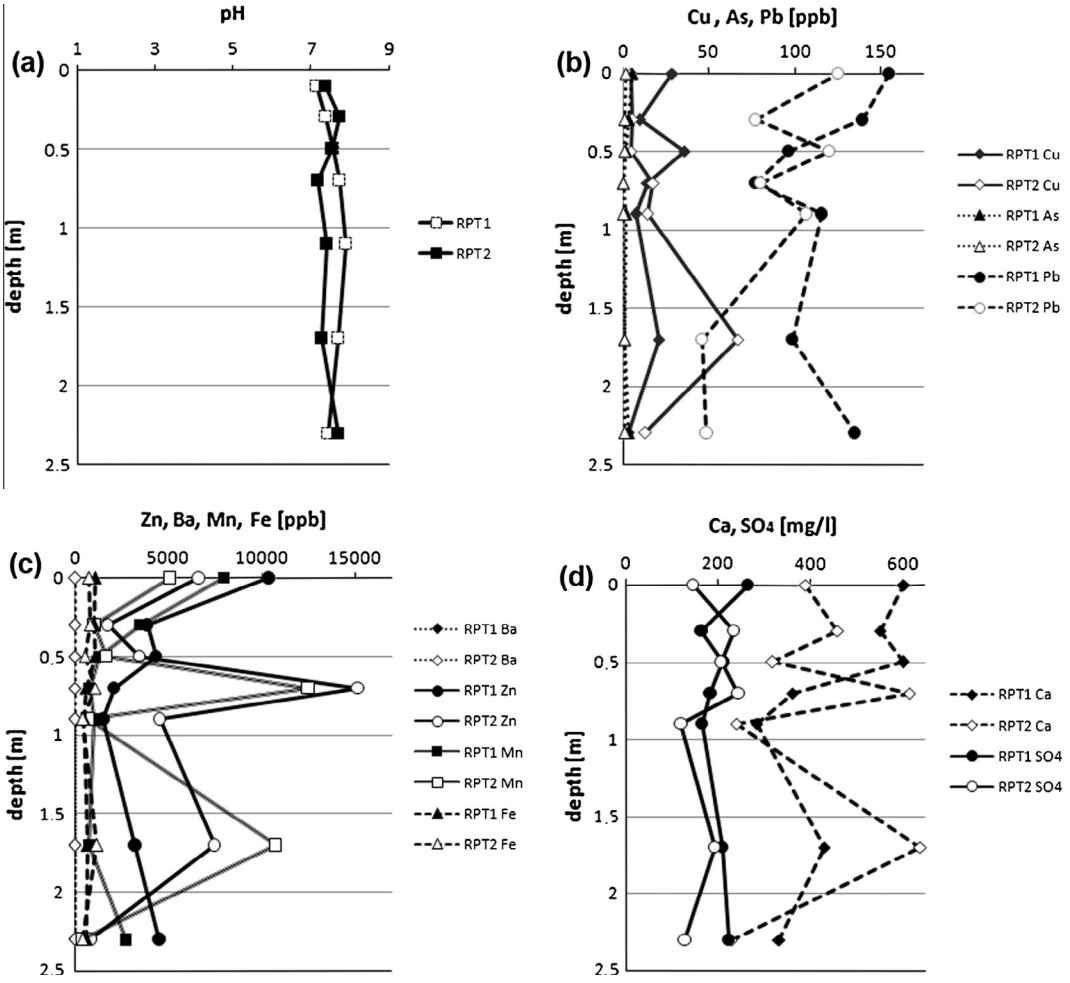

Fig. 6. Water leaching: (a) pH, (b) Cu, As, Pb, (c) Ba, Zn, Mn, Fe, (d) Ca, SO_4.

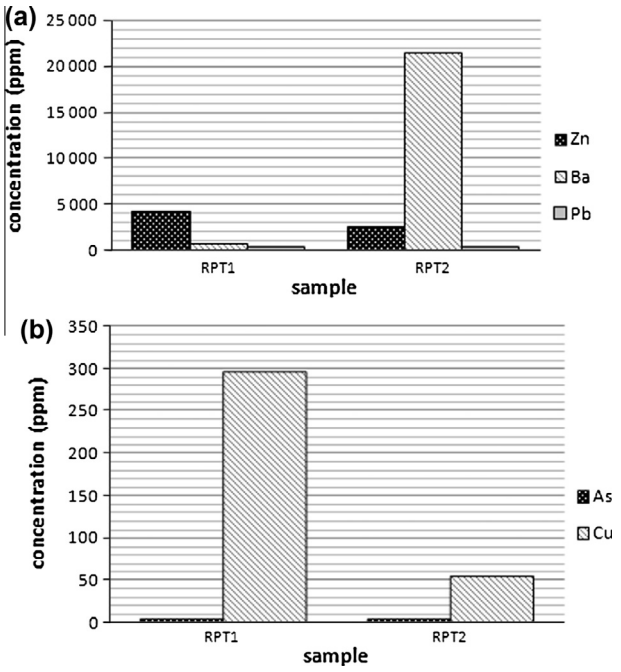

Fig. 7. Gastric leaching results: (a) Zn, Ba, Pb, (b) As, Cu.

Table 4
Gastric availability of total contaminant contents, total and gastric contents in ppm.

	Cu	Zn	As	Ba	Pb
RPT1 (total)	1,681	9,796	180	724	515
RPT1 (gastric)	297	4,160	6	627	299
RPT1 gastric (%)	17.7	42.5	3.3	86.6	58.1
RPT2 (total)	488	10,463	95	28,820	352
RPT2 (gastric)	57	2,520	5.6	21,400	252
RPT2 gastric (%)	11.7	24.1	5.9	74.3	72.0

total S may be overestimated and, thus, the NPR may be underestimated, i.e. the situation is probably more favorable than indicated by the NPR values in Fig. 2d.

Acidity and iron are produced by dissolution of pyrite. Iron precipitates in oxyhydroxides in the following global reaction:

$$FeS_2 + 3.75O_2 + 3.5H_2O = Fe(OH)_3 + 2SO_4^{2-} + 4H^+ \quad (2)$$

The resulting ferric minerals adsorb/co-precipitate Zn, Pb, Cu, and As and their coatings on the surface of primary sulfides limit their oxidation rate (Nicholson et al., 1990). Crystalline ferric phases were not identified by X-ray diffraction (Fig. 3 and Table 1), but this is not surprising when taking into account the maximum *aqua regia* Fe contents of about 32,000 ppm (3.2 wt.%) in Fig. 5a, which are below the X-ray diffraction detection limit of about 5.0 wt.%. Reducible Fe fraction contents, i.e. amorphous/low crystallinity phases are low, but the oxidizable Fe fraction contents representing unoxidized sulfides are high, (Fig. 5a), as expected in young mine tailings.

Correlation coefficients for water leaching experiments are high between Fe and Zn and Cu, but low between Fe and Pb (Table 5). Even higher correlation is observed between Mn and Zn. The aging of ferric phases in tropical semiarid climate may be relatively fast and crystalline phases such as goethite and hematite can be formed in the first year after deposition of mine tailings, as observed at the Kombat site in northeastern Namibia (Sracek et al., 2014b). Highly crystalline phases effectively immobilize contaminants such as As, e.g., in the form of surface bidentate complexes (Catalano et al., 2007). At Rosh Pinah, concentrations of water-leached Fe are relatively low, (Fig. 6c), and concentrations of leached As are very low, below 5 ppb (Fig. 6b). This indicates that As is tightly bound in ferric minerals. On the other hand, concentrations of water-leached Mn are higher than those of Fe and are followed by dissolved Zn and Cu concentrations. This suggests a link between Mn-oxyhydroxides and Zn and Cu.

In spite of the very high Ba content in solids (up to 3.0 wt.%), concentrations of water-leached Ba are low and there is a negative correlation between Ba and SO_4 (Table 5), suggesting that Ba released by dissolution of the Ba-carbonate, norsethite, precipitates in sulfate-rich pore water as barite:

$$Ba^{2+} + SO_4^{2-} = BaSO_4 \quad (3)$$

Evaporation in semiarid climate also contributes to the precipitation of secondary minerals because this process concentrates pore solutions especially close to the surface of mine tailings (Spangenberg et al., 2007; Nordstrom, 2009; Sracek et al., 2010b).

Water discharged to the southern pond is of Ca–HCO_3–SO_4 type and dissolved concentrations of metals and As are low (below 1 mg/l). However, when total concentrations are taken into account, about 74% of Zn can be present in the colloidal fraction. A significant portion of the contaminants in colloidal form was found at many other neutral mine drainage sites due to the formation of ferric colloids, which adsorb dissolved contaminants (Schemel et al., 2007; Cánovas et al., 2008; Sracek et al., 2012). Water in the pond is supersaturated with respect to barite, $Fe(OH)_3$(a), and manganite, but undersaturated with respect to any carbonate minerals. Calculated log P_{CO2} values are high as a consequence of kinetically constrained de-gassing of CO_2 produced by neutralization (Appelo and Postma, 2005). Ground water upgradient of mine tailings is of poor quality, of a Na–Cl–SO_4 type with high mineralization, and cannot be used for water supply or irrigation. There is no increase of dissolved metals in groundwater downgradient of the mine tailings, suggesting no impact of mining wastes on groundwater.

When gastric leachates are considered, gastric availability is in the order Ba > Pb > Zn > Cu > As. Gastric-available fractions are relatively high, reaching 86.6% for Ba, 72.0% for Pb, and 42.5% for

Table 5
Pearson's correlation coefficients for selected parameters in water leachates, values significant at $p = 0.05$ in bold.

	Fe	Mn	Cu	Zn	As	Ba	Pb	SO_4	Ca
Fe	1								
Mn	0.718	1							
Cu	**0.637**	**0.515**	1						
Zn	**0.632**	**0.907**	0.324	1					
As	0.331	0.199	−0.002	0.234	1				
Ba	0.084	0.219	−0.147	0.122	0.225	1			
Pb	0.010	−0.067	−0.427	0.128	**0.750**	0.245	1		
SO_4	**0.550**	0.427	0.177	0.487	0.374	−0.377	0.192	1	
Ca	**0.991**	**0.711**	**0.630**	**0.645**	0.301	−0.010	−0.004	**0.624**	1

Zn. This is consistent with the order observed by Kříbek et al. (2014), for dust fallout from the Rosh Pinah mine tailings. They found a gastric available fraction up to 85.9% for Pb, but they used much finer material blown out of mine tailings, i.e., PM_{10}, with a larger surface area and, thus, a higher reactivity. Based on water leachates, As seems to be tightly bound into ferric minerals and is not available even under gastric conditions. In contrast, as indicated by sequential extraction data, significant portions of Zn, Cu, and Pb are bound in the carbonate fraction and probably also in Mn-oxyhydroxides, which can be mobilized relatively easily under acid conditions. In summary, these results confirm previous conclusions of Meunier et al. (2010) and Jamieson (2011) about the importance of mineralogy and bioavailability determination in the evaluation of risk presented by mining wastes. On the other hand, total contaminant contents are not sufficient for risk evaluation. Crystalline ferric phases formation under tropical climate conditions may result in very low mobility of associated contaminants (Sracek et al., 2014a,b; Sracek, 2014).

6. Conclusions

The studied mine tailings at Rosh Pinah are well-neutralized with leachate pH > 7 and high NPR values. This is due to abundant dolomite in the matrix. Released Zn, Cu, and Pb are bound to Fe- and Mn-oxyhydroxides and probably also to carbonates. Fe-oxyhydroxides are very resistant to dissolution, but Mn-oxyhydroxides and carbonates are more soluble and release adsorbed and co-precipitated contaminants. Concentrations of released contaminants in water leachate follows the order Zn > Pb > Cu > As. Arsenic bound to the ferric minerals is almost immobile. Mine tailings are very rich in Ba, which is present mainly in Ba-carbonate, norsethite. However, released Ba precipitates as barite in sulfate-rich pore water and is immobile.

Dissolved concentrations in neutral mine drainage from the southern pond were in the order Cu > Zn > Pb. When total concentrations including the colloidal fraction were taken into account, more than 70% of Zn was in colloidal form. Groundwater upgradient of the mine tailings is poor quality Na–SO_4–Cl brackish water with low metal concentrations. There seems to be no negative impact on groundwater downgradient from the mine tailings.

Gastric leachate concentrations are in the order Ba > Pb > Zn > Cu > As with maximum gastric availability of 86.6% for Ba and 3.3% for As. Obtained results demonstrate the need for determination of mineralogical composition and availability of contaminants because the total content and toxicity of contaminants in the solid phase are poor predictors of environmental risk.

Acknowledgements

The funding for the study was provided by the Czech Science Foundation (GAČR P210/12/1413) and OPPK project CZ.2.16/3.1.00/21516, Youth and Sports of the Czech Republic (MSM0021620855). We thank Mr. Eric Mouton of Rosh Pinah Zinc Corporation for assistance with logistics and approval for this publication. Support for BM was via the University if Namibia Research and Publications Grant. Ms. Gisela Hinder from Rosh Pinah mine for providing us with ground water chemistry data from monitoring wells around mine tailings. We also thank two anonymous reviewers for constructive comments.

References

Alchin, D.J., Frimmel, H.E., Jacobs, L.E., 2005. Stratigraphic setting of the metalliferous Rosh Pinah Formation and the Spitzkop and Koivib Suites in the Pan-African Gariep Belt, southwestern Namibia. S. Afr. J. Geol. 108, 19–34.

Appelo, C.A.J., Postma, D., 2005. Geochemistry Groundwater and Pollution, second ed. A.A. Balkema Publishers, 649p.

ASEC (Alexandra Speiser Environmental Consultants) 2005. Environmental Management Plan & Specifications for EPLS 2616 and 2265. MS., Alexandra Speiser Environmental Consultants. Johannesburg. 45p.

Blowes, D.W., Jambor, J.L., Hanton-Fong, C.J., Lortie, L., Gould, W.D., 1998. Geochemical, mineralogical and microbiological characterization of a sulphide-bearing, carbonate-rich gold-mine tailings impoundment, Joutel, Québec. Appl. Geochem. 13 (6), 687–705.

Blowes, D.W., Ptacek, C.J., Jambor, J.L., Weisener, C.G., 2003. The geochemistry of acid mine drainage. In: Lollar, B.S. (Ed.), Environmental Geochemistry, Treatise on Geochemistry, vol. 9. Elsevier, pp. 149–204.

Cánovas, C.R., Hubbard, C.G., Olias, M., Nieto, J.M., Black, S., Coleman, M.L., 2008. Hydrochemical variations and contaminant load in the Río Tinto (Spain) during flood events. J. Hydrol. 350 (1–2), 25–40.

Catalano, J.G., Zhang, Z., Park, C., Fentner, P., Bedzyk, M.J., 2007. Bridging arsenate surface complexes on the hematite (012) surface. Geochim. Cosmochim. Acta 71, 1883–1897.

Dold, B., 2010. Basic concepts in environmental geochemistry of sulfidic mine-waste management. In: Kumar, E.S. (Ed.), Waste Management. INTECH, Croatia, pp. 173–198.

Dold, B., Fontboté, L., 2001. Element cycling and secondary mineralogy in porphyry copper tailings as a function of climate, primary mineralogy, and mineral processing. J. Geochem. Explor. 74, 3–55.

Ettler, V., Kříbek, B., Majer, V., Knésl, I., Mihaljevič, 2012. Differences in the bioaccessibility of metal/metalloids in soils from mining and smelting areas (Copperbelt, Zambia). J. Geochem. Explor. 113, 68–75.

Gasser, U.G., Walker, W.J., Dahlgren, R.A., Borch, R.S., Burau, R.G., 1996. Lead release from smelter and mine waste impacted material under simulated gastric conditions and relation to speciation. Environ. Sci. Technol. 30, 761–769.

Hossner, L.R., Doolittle, J.L., 2003. Iron sulfidic oxidation as influenced by calcium carbonate application. J. Environ. Qual. 32, 773–780.

Jambor, J.L., 2003. Mine-waste mineralogy and mineralogical perspectives on acid–base accounting, In: Jambor J.L., Blowes D.W., Ritchie A.I.M. (Eds.), Environmental Aspects of Mine Wastes, Short Course Series, vol. 31, Mineralogical Association of Canada, pp. 117–145.

Jamieson, H.E., 2011. Geochemistry and mineralogy of solid mine waste: essential knowledge for predicting environmental impact. Elements 7, 381–386.

Kříbek, B., Majer, V., Pašava, J., Kamona, F., Mapani, B., Keder, J., Ettler, V., 2014. Contamination of soils with dust fallout from the tailings dam at the Rosh Pinah area, Namibia: Regional assessment, dust dispersion modelling and environmental consequences. J. Geochem. Explor. 144 (Part C), 391–408.

Lindsey, M.B.J., Condon, P.D., Jambor, J.J., Lear, K.G., Blowes, D.W., Ptacek, C.J., 2009. Mineralogical, geochemical, and microbial investigation of a sulfide-rich tailings deposit characterized by neutral drainage. Appl. Geochem. 24, 2212–2221.

McGregor, R.G., Blowes, D.W., 2002. The physical, chemical and mineralogical properties of three cemented layers within sulfide-bearing mine tailings. J. Geochem. Explor. 76, 195–207.

Meunier, L., Walker, S.R., Wragg, J., Parson, M.B., Koch, I., Jamieson, H.E., Reimer, K.J., 2010. Effects of soil composition and mineralogy on the Bioaccessibility of arsenic from mine tailings and soil in gold mine district of Nova Scotia. Environ. Sci. Technol. 44, 2667–2674.

Nicholson, R.V., Gillham, R.W., Reardon, E.J., 1990. Pyrite oxidation in carbonate buffered solution: 2. Rate control by oxide coatings. Geochim. Cosmochim. Acta 54, 395–402.

Nordstrom, D.K., 2009. Acid rock drainage and climatic change. J. Geochem. Explor. 100, 97–104.

Ondruš, P., 1993. ZDS – a Computer Program for Analysis of X-ray Powder Diffraction Patterns. Materials Science Forum, pp. 133–136. 297–300, EPDIC-2. Enchede.

Parkhurst, D.L., Appelo, C.A.J., 1999. User's Guide to PHREEQC; a Computer Program for Speciation, Reaction-path, 1-D Transport and Inverse Geochemical Calculations, U.S. Geological Survey Water Resources-Investigations Report 99-4259.

Plumlee, G.S., Ziegler, T.L., 2006. The medical geochemistry of dusts, soils and other earth materials. Treatise Geochem. 9, 263–310.

Rauret, G., Lopez-Sanchez, J.F., Sahuquillo, A., Rubio, R., Davidson, C., Ure, A., Quevauviller, P., 1999. Improvement of the BCR three step sequential extraction procedure prior to the certification of new sediment and soil reference materials. J. Environ. Monit. 1, 57–61.

Romero, F.M., Armienta, M.A., Villasenor, G., Gonzáles, J.L., 2006. Mineralogical constraints on the mobility of arsenic in tailings from Zimapán, Hidalgo, Mexico. Int. J. Environ. Pollut. 26, 23–40.

Romero, F.M., Villalobos, M., Aguirre, R., Gutierrez, M.E., 2008. Solid-phase control on lead bioaccessibility in smelter-impacted soils. Arch. Environ. Contam. Toxicol. 55 (4), 566–575.

Roussel, H., Waterlot, C., Pefrene, A., Pruvot, C., Mazzuca, M., Douay, F., 2010. Cd, Pb and Zn bioaccessibility of urban soils contaminate din the past by atmospheric emissions from two lead and zinc smelters. Arch. Environ. Contam. Toxicol. 58, 945–954.

Ruby, M.V., Schoof, R., Brattin, W., Goldade, M., Post, G., Hranois, M., Mosby, D.E., Casteel, S.W., Berti, W., Carpenter, M., Edwards, D., Cragin, D., Chapell, W., 1999. Advances in evaluating the oral bioavailability of inorganics in soil use in human health risk assessment. Environ. Sci. Technol. 33, 2697–3705.

Schemel, L.E., Kimball, B.A., Runkel, R.L., Cox, M.H., 2007. Formation of mixed Al–Fe colloidal sorbent and dissolved-colloidal partitioning of Cu and Zn in the Cement Creek – Animas River Confluence, Silverton, Colorado. Appl. Geochem. 22 (7), 1467–1484.

Spangenberg, J.E., Dold, B., Vogt, M.-L., Pfeifer, H.-R., 2007. Stable hydrogen and oxygen isotope composition of water from mine tailings in different climatic environments. Environ. Sci. Technol. 41, 1870–1876.

Sracek, O., 2014. Formation of secondary hematite and its role in attenuation of contaminants at mine tailings: review and comparison of sites in Zambia and Namibia. Front. Environ. Sci. 2 (64), 1–11.

Sracek, O., Mihaljevič, M., Kříbek, B., Majer, V., Veselovský, F., 2010a. Geochemistry and mineralogy of Cu and Co in mine tailings at the Copperbelt, Zambia. J. African Earth Sci. 57, 14–30.

Sracek, O., Veselovský, F., Kříbek, B., Malec, J., Jehlička, J., 2010b. Geochemistry, mineralogy and environmental impact of precipitated efflorescent salts at the Kabwe Cu- Co chemical leaching plant in Zambia. Appl. Geochem. 25, 1815–1824.

Sracek, O., Kříbek, B., Mihaljevič, M., Majer, V., Veselovský, F., Vencelides, Z., Nyambe, I., 2012. Mining-related contamination of surface water and sediments of the Kafue River drainage system in the Copperbelt district, Zambia: An example of a high neutralization capacity system. J. Geochem. Explor. 112, 174–188.

Sracek, O., Mihaljevič, M., Kříbek, B., Majer, V., Filip, J., Vaněk, A., Penížek, V., Ettler, V., Mapani, B., 2014a. Geochemistry and mineralogy of vanadium in mine tailings at Berg Aukas, northeastern Namibia. J. Afr. Earth Sc. 96, 180–189.

Sracek, O., Mihaljevič, M., Kříbek, B., Majer, V., Filip, J., Vaněk, A., Penížek, V., Ettler, V., Mapani, B., 2014b. Geochemistry of mine tailings and behavior of arsenic at Kombat, northeastern Namibia. Environ. Monit. Assess. 186, 4891–4903.

US EPA, 2007. Estimation of Relative Bioavailability of Lead in Soil and Soil-like Materials Using *in vivo* and *in vitro* Methods, Office of Solid Waste and Emergency Response, US EPA, Washington, OSWER 9285.7-77.

van Vuuren, C.J.J., 1986. Regional setting and structure of the Rosh Pinah Zinc-Lead deposit, South West Africa/Namibia. In: Wilson, M.G.C., Anhaeusser, C.R. (Eds.), Mineral Deposits of Southern Africa. Council for Geoscience, Pretoria, pp. 1593–1607.